Improved Standard-Model Prediction for $\pi^0 \to e^+e^-$

Martin Hoferichter,[1] Bai-Long Hoid,[1] Bastian Kubis,[2] and Jan Lüdtke[2,3]
[1]Albert Einstein Center for Fundamental Physics, Institute for Theoretical Physics, University of Bern, Sidlerstrasse 5, 3012 Bern, Switzerland
[2]Helmholtz-Institut für Strahlen- und Kernphysik and Bethe Center for Theoretical Physics, Universität Bonn, 53115 Bonn, Germany
[3]Faculty of Physics, University of Vienna, Boltzmanngasse 5, 1090 Vienna, Austria

(Received 13 May 2021; revised 18 August 2021; accepted 25 March 2022; published 29 April 2022)

We present an improved standard-model (SM) prediction for the dilepton decay of the neutral pion. The loop amplitude is determined by the pion transition form factor for $\pi^0 \to \gamma^*\gamma^*$, for which we employ a dispersive representation that incorporates both spacelike and timelike data as well as short-distance constraints. The resulting SM branching fraction, $\mathrm{Br}[\pi^0 \to e^+e^-] = 6.25(3) \times 10^{-8}$, sharpens constraints on physics beyond the SM, including pseudoscalar and axial-vector mediators.

DOI: 10.1103/PhysRevLett.128.172004

Introduction.—The decay of the neutral pion proceeds almost exclusively into two photons, with the decay mediated by the Wess-Zumino-Witten anomaly [1,2]. The decay width

$$\Gamma[\pi^0 \to \gamma\gamma] = \frac{\pi\alpha^2 M_{\pi^0}^3}{4} F_{\pi\gamma\gamma}^2 \tag{1}$$

depends on the pion transition form factor (TFF) at zero momentum transfer, $F_{\pi\gamma\gamma} = F_{\pi^0\gamma^*\gamma^*}(0,0)$, which in turn is determined by a low-energy theorem [3–5]

$$F_{\pi\gamma\gamma} = \frac{1}{4\pi^2 F_\pi} = 0.2745(3)\ \mathrm{GeV}^{-1}, \tag{2}$$

in terms of the pion decay constant $F_\pi = 92.28(10)$ MeV [6]. This prediction agrees extremely well with experiment, $F_{\pi\gamma\gamma} = 0.2754(21)\ \mathrm{GeV}^{-1}$ [7], despite the fact that at this level higher-order corrections are expected [8–11]. The second most important decay channel is the Dalitz decay $\pi^0 \to e^+e^-\gamma$. Combining the radiative corrections from Ref. [12] with phenomenological input on the slope of the TFF [13–20] gives [21]

$$\mathrm{Br}[\pi^0 \to \gamma\gamma] = 98.8131(6)\%, \tag{3}$$

in agreement with but more precise than the direct measurement $\mathrm{Br}[\pi^0 \to \gamma\gamma] = 98.823(34)\%$ [6,22–24]. The decay $\pi^0 \to 2(e^+e^-)$ is suppressed by another factor of α with respect to the Dalitz decay, leading to $\mathrm{Br}[\pi^0 \to 2(e^+e^-)] = 3.26(18) \times 10^{-5}$ [25].

Here, we are interested in the rare decay $\pi^0 \to e^+e^-$, whose dominant contribution in the standard model (SM) arises from the loop diagram shown in Fig. 1. Apart from a loop factor, there is yet another chiral suppression, which is partly lifted by logarithmic corrections. Altogether, this leads to the scaling [26]

$$\mathrm{Br}[\pi^0 \to e^+e^-] \sim \left(\frac{\alpha}{\pi}\right)^2 \frac{m_e^2}{M_{\pi^0}^2} \pi^2 \log^2 \frac{m_e}{M_{\pi^0}} \sim \mathcal{O}(10^{-8}), \tag{4}$$

and due to the corresponding suppression the decay has been suggested early on to search for physics beyond the SM (BSM) [27]. Since the interference with the Z-boson contribution, see second diagram in Fig. 1, is suppressed by another 2 orders of magnitude [28–30], sensitivity to BSM degrees of freedom in general requires a precision measurement of $\mathrm{Br}[\pi^0 \to e^+e^-]$, unless the BSM contribution is enhanced in one way or another. Such an enhancement could originate from avoiding the chiral suppression in Eq. (4) via pseudoscalar operators, or by considering light degrees of freedom, such as axial-vector Z' bosons [31,32] or axionlike particles [33–38].

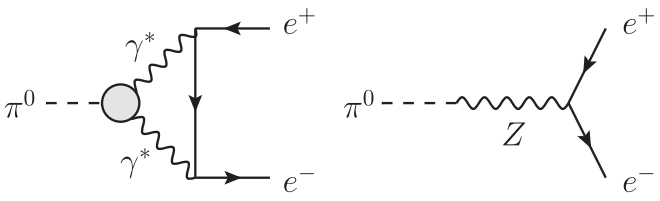

FIG. 1. SM contributions to $\pi^0 \to e^+e^-$, with the dominant $\pi^0 \to \gamma^*\gamma^*$ diagram (left) and a small correction from Z exchange (right). The gray blob refers to the pion TFF.

The current best measurement by the KTeV experiment constrains $\mathrm{Br}[\pi^0 \to e^+e^-]$ at the level of 5% [39], but the interpretation is complicated by the fact that the result is provided with a cut on the dilepton invariant mass, which needs to be extrapolated to obtain the full branching fraction. Using the latest radiative corrections from Refs. [40,41], one finds

$$\mathrm{Br}[\pi^0 \to e^+e^-]|_{\mathrm{KTeV}} = 6.85(27)(23) \times 10^{-8}, \quad (5)$$

significantly lower than the extrapolation $\mathrm{Br}[\pi^0 \to e^+e^-] = 7.48(38) \times 10^{-8}$ given in Ref. [39] based on the radiative corrections from Ref. [42] (see also Ref. [43]), with the difference due to the assumption of a pointlike $\pi^0 \to e^+e^-$ vertex in Ref. [42]. We used the total correction $\delta = -6.0(2)\%$ in Eq. (5), in line with the low-energy constant $\chi^{(r)}(\mu = 0.77\ \mathrm{GeV}) = 2.69(10)$ that corresponds to our result for the pion TFF [40,41,44], see below. Note that precisely due to the potentially complicated dependence on kinematical cuts, we follow the convention to subtract the radiative corrections from the experimental result and use the leading order in QED as the reference point for comparison between theory and experiment.

In the SM prediction, the imaginary part of the amplitude due to the $\gamma\gamma$ cut is determined model independently in terms of $\Gamma[\pi^0 \to \gamma\gamma]$, leading to a unitarity bound of $\mathrm{Br}[\pi^0 \to e^+e^-] > 4.69 \times 10^{-8}$ [45,46]. To obtain the real part, additional information needs to be provided on the TFF, see Ref. [47] for a review. Chiral perturbation theory (CHPT) only allows one to relate the dilepton decays of π^0 and $\eta^{(\prime)}$, but cannot predict $\mathrm{Br}[\pi^0 \to e^+e^-]$ itself [48,49]. Further approaches that have been pursued instead include vector-meson-dominance TFFs [50–53] and a dispersion relation in the pion mass squared [54–58]. However, we stress that such a dispersion relation is model dependent, as the TFF for unphysical masses is not observable, and the input for the imaginary part is typically restricted to the $\gamma\gamma$ cut.

More recent SM predictions include $\mathrm{Br}[\pi^0 \to e^+e^-] = 6.23(5) \times 10^{-8}$ [29] based on Canterbury approximants and $\mathrm{Br}[\pi^0 \to e^+e^-] = 6.22(3) \times 10^{-8}$ [59] (excluding Z exchange) using Dyson-Schwinger equations [60]. The Canterbury expansion relies on spacelike data for the pion TFF [18,61–63] and is, in principle, systematically improvable, but in practice restricted due to the available data, especially the lack thereof in the doubly virtual direction, while for the Dyson-Schwinger approach a complete estimate of the truncation uncertainties is challenging. The $\pi^0 \to e^+e^-$ decay is also becoming amenable to calculations in lattice QCD [64].

In this Letter, we present a SM prediction that is based on a dispersive representation of the pion TFF first developed in the context of the pion-pole contribution [13–15] in a dispersive approach to hadronic light-by-light scattering [65–71], with further applications to hadronic vacuum polarization [72,73]. In the dispersive approach presented here we are able to implement constraints from all available low-energy data, including the timelike region, to predict the doubly virtual behavior from singly virtual data, and to ensure a smooth matching to short-distance constraints. The resulting SM prediction, which is as precise as we believe can currently be achieved with data-driven methods, is then used to sharpen some of the constraints that can be extracted from the comparison to the KTeV measurement. We also clarify some technical points in the calculation of the SM amplitude, and show that a Wick rotation to spacelike momenta is possible once a double-spectral representation is employed for the pion TFF.

Pion transition form factor.—The pion TFF is defined by the matrix element of two electromagnetic currents $j_\mu(x)$

$$\begin{aligned} &i \int d^4x e^{iq_1\cdot x} \langle 0|T\{j_\mu(x) j_\nu(0)\}|\pi^0(q_1+q_2)\rangle \\ &\quad = \epsilon_{\mu\nu\alpha\beta} q_1^\alpha q_2^\beta F_{\pi^0\gamma^*\gamma^*}(q_1^2, q_2^2), \end{aligned} \quad (6)$$

where we follow the sign conventions of Refs. [74–76] to ensure consistency with the short-distance constraints and the Z-boson contribution. This form factor has been studied in great detail in the context of hadronic light-by-light scattering [14,15,17,77], the key difference being that in this case the loop integral can be Wick rotated to spacelike momenta for an arbitrary TFF [78]. In the case of $\pi^0 \to e^+e^-$ the analogous master formula becomes more intricate, so before turning to this application we first describe the representation we will use for the normalized TFF $\tilde{F}_{\pi^0\gamma^*\gamma^*}(q_1^2, q_2^2) = F_{\pi^0\gamma^*\gamma^*}(q_1^2, q_2^2)/F_{\pi\gamma\gamma}$ in the following. We use the decomposition

$$\tilde{F}_{\pi^0\gamma^*\gamma^*} = \tilde{F}^{\mathrm{disp}}_{\pi^0\gamma^*\gamma^*} + \tilde{F}^{\mathrm{eff}}_{\pi^0\gamma^*\gamma^*} + \tilde{F}^{\mathrm{asym}}_{\pi^0\gamma^*\gamma^*}, \quad (7)$$

where the dispersive term accounts for the low-energy singularities, extracted from data on $e^+e^- \to 2\pi, 3\pi$; the second term parametrizes the small effect from higher intermediate states and high-energy contributions, it enforces the correct normalization and is further constrained by high-energy spacelike data; and the third term implements the remaining short-distance constraints as expected from perturbative QCD.

In practice, the dispersive part is written as a double-spectral representation (exploiting the absence of anomalous thresholds in this case [68,79])

$$\begin{aligned} \tilde{F}^{\mathrm{disp}}_{\pi^0\gamma^*\gamma^*}(q_1^2, q_2^2) &= \frac{1}{\pi^2} \int_{4M_\pi^2}^{s_{\mathrm{iv}}} dx \int_{s_{\mathrm{thr}}}^{s_{\mathrm{is}}} dy \frac{\tilde{\rho}(x,y)}{(x-q_1^2)(y-q_2^2)} \\ &\quad + (q_1 \leftrightarrow q_2), \\ \tilde{\rho}(x,y) &= \frac{q_\pi^3(x)}{12\pi\sqrt{x} F_{\pi\gamma\gamma}} \mathrm{Im}\{[F_\pi^V(x)]^* f_1(x,y)\}, \end{aligned} \quad (8)$$

with $q_\pi(s) = \sqrt{s/4 - M_\pi^2}$, and $s_{\mathrm{thr}} = 9M_\pi^2$ or $M_{\pi^0}^2$ depending on whether isospin-breaking corrections are included.

The double-spectral density $\tilde{\rho}(x,y)$ is determined by the electromagnetic form factor of the pion, F_π^V, and the P-wave amplitude for $\gamma^* \to 3\pi$, f_1. The former is known very precisely from $e^+e^- \to 2\pi$ data (see, e.g., Refs. [80,81]), while the latter can be obtained from a solution of Khuri-Treiman equations [82], with free parameters determined from $e^+e^- \to 3\pi$ data [13–15]. The integration cutoffs are varied between 1.8 and 2.5 GeV, which, together with the variations of the $\pi\pi$ phase shifts and the conformal polynomial in the partial wave f_1, defines the dispersive contribution to the uncertainty estimate.

The unsubtracted dispersion relation (8) only saturates the normalization at the level of 90%, with the remainder restored by an effective-pole contribution,

$$\tilde{F}^{\text{eff}}_{\pi^0\gamma^*\gamma^*}(q_1^2,q_2^2) = g_{\text{eff}}\frac{M_{\text{eff}}^4}{(M_{\text{eff}}^2-q_1^2)(M_{\text{eff}}^2-q_2^2)}, \quad (9)$$

that accounts for higher intermediate states beyond 2π, 3π as well as the high-energy part of the integrals. The coupling g_{eff} follows from the normalization, while the mass scale M_{eff} is determined from a fit to the singly virtual spacelike data [18,61–63] with $Q^2 > 5\ \text{GeV}^2$, to ensure that the low-energy properties remain unaffected. The resulting value of M_{eff} lies in the range 1.5–2 GeV, with an uncertainty dominated by the systematic tension between the *BABAR* Collaboration data [62] and the other data sets, as well as the Brodsky-Lepage (BL) limit [83,84].

Finally, the asymptotic contribution

$$\tilde{F}^{\text{asym}}_{\pi^0\gamma^*\gamma^*}(q_1^2,q_2^2) = \frac{2F_\pi}{F_{\pi\gamma\gamma}}\int_{s_m}^{\infty} dx \frac{q_1^2 q_2^2}{(x-q_1^2)^2(x-q_2^2)^2} \quad (10)$$

ensures the correct asymptotic behavior for nonvanishing virtualities, and has been derived by expressing the short-distance constraints in terms of a dispersion relation [14,15,85,86]. The matching point is chosen as $s_m = 1.7(3)\ \text{GeV}^2$, in accordance with expectations from light-cone sum rules [85,87,88]. The resulting TFF that emerges from the sum in Eq. (7) is illustrated in Fig. 2 for the kinematic configuration most relevant for $\pi^0 \to e^+e^-$, demonstrating that our representation smoothly connects the various constraints on the pion TFF.

SM prediction for $\pi^0 \to e^+e^-$.—The normalized branching fraction for $\pi^0 \to e^+e^-$,

$$\frac{\text{Br}[\pi^0 \to e^+e^-]}{\text{Br}[\pi^0 \to \gamma\gamma]} = 2\sigma_e(q^2)\left(\frac{\alpha}{\pi}\right)^2 \frac{m_e^2}{M_{\pi^0}^2}|\mathcal{A}(q^2)|^2, \quad (11)$$

is typically expressed in terms of the reduced amplitude

$$\mathcal{A}(q^2) = \frac{2i}{\pi^2 q^2}\int d^4k \frac{q^2k^2-(q\cdot k)^2}{k^2(q-k)^2[(p-k)^2-m_e^2]} \times \tilde{F}_{\pi^0\gamma^*\gamma^*}[k^2,(q-k)^2], \quad (12)$$

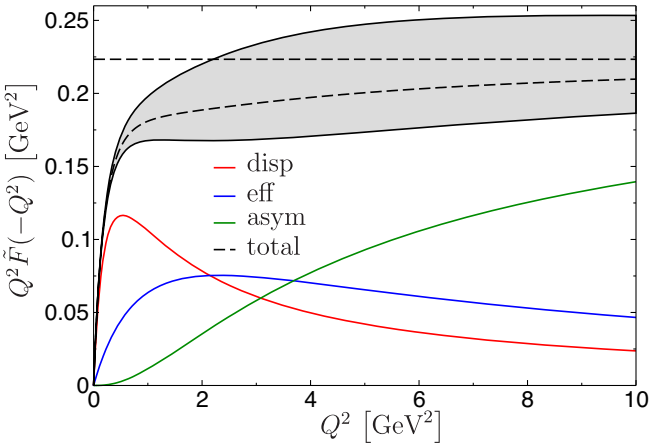

FIG. 2. Dispersive, effective-pole, and asymptotic contributions to the pion TFF, using the representation from [89] with $\tilde{k}^2 \to -Q^2$. This form factor $\tilde{F}(-Q^2)$ defines a single-variable function that is closely related to the input required for a spacelike evaluation of the loop integral, for which $\tilde{F}_{\pi^0\gamma^*\gamma^*}(-Q^2,-Q^2)$ is not sufficient. In particular, due to the $M_{\pi^0}^2$ corrections, the form factor $\tilde{F}(-Q^2)$ is not normalized exactly to unity at $Q^2 = 0$. The gray band indicates our uncertainty estimate, the horizontal dashed line the asymptotic value $2F_\pi/(3F_{\pi\gamma\gamma})$.

where $q^2 = M_{\pi^0}^2$ and p is the momentum of the outgoing electron. The only imaginary part arises from the $\gamma\gamma$ cut, which leads to

$$\text{Im}\ \mathcal{A}(q^2) = \frac{\pi}{2\sigma_e(q^2)}\log[y_e(q^2)] = -17.52,$$
$$y_e(q^2) = \frac{1-\sigma_e(q^2)}{1+\sigma_e(q^2)}, \quad \sigma_e(q^2) = \sqrt{1-\frac{4m_e^2}{q^2}}, \quad (13)$$

and defines the unitarity bound given above.

To obtain Re $\mathcal{A}(q^2)$ we need to perform the integral (12) for our representation of the pion TFF. For the dispersive part one may write

$$\mathcal{A}^{\text{disp}}(q^2) = \frac{2}{\pi^2}\int_{4M_\pi^2}^{s_{\text{iv}}} dx \int_{s_{\text{thr}}}^{s_{\text{is}}} dy \frac{\tilde{\rho}(x,y)}{xy}K(x,y), \quad (14)$$

where the integration kernel

$$K(x,y) = \frac{2i}{\pi^2 q^2}\int d^4k \frac{q^2k^2-(q\cdot k)^2}{k^2(q-k)^2[(p-k)^2-m_e^2]} \times \frac{xy}{(k^2-x)[(q-k)^2-y]} \quad (15)$$

can be evaluated based on standard loop functions, see Refs. [30,89–91]. The effective-pole contribution follows from $x = y = M_{\text{eff}}^2$, and a similar decomposition can be derived for $\mathcal{A}^{\text{asym}}(q^2)$. The numerical integration over the double-spectral function requires a stable implementation of $K(x,y)$ over a wide parameter range, especially in view

of the singularity structure of $f_1(x,y)$ that needs to be properly taken into account. As discussed in [89], we verified the numerical stability by comparing several different methods, in particular, a Wick rotation to spacelike momenta. Such a Wick rotation is not possible for a completely general TFF, but does apply for the double-spectral representation. Combining first the photon propagators, the angular part of the integral can be performed analytically with the method of Gegenbauer polynomials [92–94], leaving an integration over a spacelike modulus. In practice, however, we do not use this implementation of the loop functions, as it proves numerically less viable than other methods, including semianalytic expressions in terms of polylogarithms [95] and the implementation from LoopTools [96].

In the end, we find for the long-range contribution

$$\text{Re}\ \mathcal{A}(q^2)|_{\gamma^*\gamma^*} = 10.16(5)_{\text{disp}}(8)_{\text{BL}}(2)_{\text{asym}}, \tag{16}$$

with an uncertainty dominated by the systematic tensions around the BL limit. For comparison we quote $\mathcal{A}(q^2)|_{\gamma^*\gamma^*} = 10.10(3) - 17.45(1)i$ [59] and $\text{Re}\ \mathcal{A}(q^2)|_{\gamma^*\gamma^*} = 10.08(16)$ reconstructed from the decay rate given in Ref. [29]. The full number decomposes as $10.16 = 9.18_{\text{disp}} + 1.08_{\text{eff}} - 0.10_{\text{asym}}$ according to the three terms in Eq. (7), reflecting the hierarchy expected from Fig. 2. Matching to CHPT

$$\text{Re}\ \mathcal{A}(q^2)|_{\text{CHPT}} = \frac{\text{Li}_2[-y_e(q^2)] + \frac{1}{4}\log^2[y_e(q^2)] + \frac{\pi^2}{12}}{\sigma_e(q^2)} + 3\log\frac{m_e}{\mu} - \frac{5}{2} + \chi^{(r)}(\mu) \tag{17}$$

then also determines the low-energy constant $\chi^{(r)}(\mu = 0.77\ \text{GeV}) = 2.69(10)$ (see, e.g., Refs. [15,41] for the conventions).

At this level of precision the contribution from the asymptotic region thus needs to be included, as does the Z-boson exchange [30]

$$\text{Re}\ \mathcal{A}(q^2)|_Z = -\frac{F_\pi G_F}{\sqrt{2}\alpha^2 F_{\pi\gamma\gamma}} = -0.05(0). \tag{18}$$

Adding both contributions, we obtain the SM prediction

$$\begin{aligned} \text{Re}\ \mathcal{A}(q^2)|_{\text{SM}} &= 10.11(10), \\ \text{Br}[\pi^0 \to e^+e^-]|_{\text{SM}} &= 6.25(3) \times 10^{-8}, \end{aligned} \tag{19}$$

in a mild 1.8σ tension with the KTeV measurement (5). In particular, the latter implies

$$\text{Re}\ \mathcal{A}(q^2)|_{\text{KTeV}} = 11.89^{+0.94}_{-1.02}, \tag{20}$$

which, in comparison to Eq. (19), can directly be used to constrain effects beyond the SM.

Constraints on BSM physics.—The comparison between our improved SM prediction (19) and the KTeV measurement (20) sharpens the constraints on physics beyond the SM. Writing new short-range interactions of axial-vector and pseudoscalar type as

$$\mathcal{L}^{(1)}_{\text{BSM}} = C_A \bar{q}\frac{\tau^3}{2}\gamma^\mu\gamma_5 q \bar{e}\gamma_\mu\gamma_5 e + C_P \bar{q}\frac{\tau^3}{2} i\gamma_5 q \bar{e} i\gamma_5 e, \tag{21}$$

with $q = (u,d)^T$, we obtain

$$\text{Re}\ \mathcal{A}(q^2)|_{\text{BSM}} = -\frac{F_\pi}{\alpha^2 F_{\pi\gamma\gamma}}\left(C_A + \frac{M^2_{\pi^0}}{4 m_e \hat{m}} C_P\right), \tag{22}$$

where $\hat{m} = (m_u + m_d)/2$, cf. also Refs. [29,30,97]. In particular, integrating out Z exchange in the SM gives $C_A = G_F/\sqrt{2}$, in agreement with Eq. (18).

The limits derived from $\pi^0 \to e^+e^-$ are

$$C_A = (-280)^{+160}_{-150}\ \text{TeV}^{-2}, \quad C_P = (-0.108)^{+0.062}_{-0.057}\ \text{TeV}^{-2}, \tag{23}$$

where the pseudoscalar coefficient has been evaluated at the $\overline{\text{MS}}$ scale $\mu = 2$ GeV using $\hat{m} = 3.4$ MeV [98–103]. Assuming $C_{A,P} \sim 1/\Lambda^2_{A,P}$, the sensitivity of these limits translates to mass scales $\Lambda_A \sim 0.1$ TeV, $\Lambda_P \sim 4$ TeV, reflecting the enhancement by $M_{\pi^0}/(2\sqrt{m_e \hat{m}}) \sim 50$, although the latter is a scale-dependent statement. Matching onto four-fermion operators in SM effective field theory [104,105], Eq. (23) provides constraints for

$$\begin{aligned} C_A &= \frac{1}{4}(C_{eu} - C_{ed} - C_{\ell u} + C_{\ell d} - 2C^{(3)}_{\ell q}), \\ C_P &= \frac{1}{4}(C^{(1)}_{\ell equ} - C_{\ell edq}). \end{aligned} \tag{24}$$

While the one for C_A is not very stringent, the combination of Wilson coefficients differs from the ones probed in parity-violating electron scattering or atomic parity violation, in such a way that the resulting constraint may still be useful to close flat directions in the parameter space, see, e.g., Refs. [106–108].

Other BSM scenarios include light axial-vector (Z') or pseudoscalar (a) states, with minimal couplings

$$\mathcal{L}^{(2)}_{\text{BSM}} = \sum_{f=e,u,d} \bar{f}(c^f_A \gamma^\mu\gamma_5 Z'_\mu + c^f_P i\gamma_5 a) f, \tag{25}$$

leading to

$$C_A = -\frac{(c^u_A - c^d_A)c^e_A}{M^2_{Z'}}, \qquad C_P = \frac{(c^u_P - c^d_P)c^e_P}{m^2_a - q^2}, \tag{26}$$

where the new particles correspond to a Z' or an axionlike particle a, respectively. Writing the Z' interactions in a gauge-invariant way in general requires the introduction of Goldstone modes, so that in Eq. (26) and below we use

unitary gauge to make the particle content explicit. In this way, the pole in C_A cancels and the SM Z contribution is again recovered for $c_A^u = -c_A^d = -c_A^e = g/(4\cos\theta_W)$. In contrast, the pseudoscalar pole remains, and the constraints from $\pi^0 \to e^+e^-$ then also depend on the π^0–a mixing.

As an application, we consider the interplay with the anomalous magnetic moment of the electron a_e, which is timely given the current tensions between the direct measurement [109] and the SM prediction [110,111] either based on the fine-structure constant measured with Cs [112] or Rb [113] atom interferometry

$$\Delta a_e[\mathrm{Cs}] = a_e^{\mathrm{exp}} - a_e^{\mathrm{SM}}[\mathrm{Cs}] = -0.88(36) \times 10^{-12},$$
$$\Delta a_e[\mathrm{Rb}] = a_e^{\mathrm{exp}} - a_e^{\mathrm{SM}}[\mathrm{Rb}] = 0.48(30) \times 10^{-12}, \qquad (27)$$

corresponding to a tension of -2.5σ and $+1.6\sigma$, respectively. With the 5.4σ disagreement between Refs. [112,113] unresolved, we will concentrate here on the case of $\Delta a_e[\mathrm{Cs}]$, since a negative effect can be explained by axial-vector or pseudoscalar mediators [114,115]

$$a_e^A = -\frac{(c_A^e)^2 m_e^2}{4\pi^2 M_{Z'}^2} \int_0^1 dx \frac{2x^3 m_e^2 + x(1-x)(4-x)M_{Z'}^2}{m_e^2 x^2 + M_{Z'}^2(1-x)},$$
$$a_e^P = -\frac{(c_P^e)^2 m_e^2}{8\pi^2} \int_0^1 dx \frac{x^3}{m_e^2 x^2 + m_a^2(1-x)}, \qquad (28)$$

while, at the one-loop level, vector and scalar mediators yield a positive contribution. For the axial-vector case, the contour plot revises the previously preferred region [32,112] according to our improved SM prediction and the radiative corrections [40,41] applied to the KTeV measurement, see Fig. 3. The parameter regions favored by $\Delta a_e[\mathrm{Cs}]$ and $\pi^0 \to e^+e^-$ partly overlap, in which case the quark couplings $c_{A,P}^u - c_{A,P}^d$ take similar values as the electron ones. Note that in Refs. [32,112] specific values for the quark couplings have been assumed to show the constraints solely on c_A^e; see these references for other constraints on axial-vector Z' models, e.g., from e^+e^- colliders [116]. We have further restricted the masses to the parameter region below M_{π^0}, and neglected the potential π^0–a mixing (as before, the pseudoscalar couplings are evaluated at the $\overline{\mathrm{MS}}$ scale $\mu = 2$ GeV). Figure 3 shows that if both mild tensions were confirmed at this level, similar regions in parameter space seem to be preferred.

Conclusions.—In this Letter, we presented an improved SM prediction for the $\pi^0 \to e^+e^-$ decay, based on a dispersive representation of the pion transition form factor. This representation—which combines constraints from $\pi^0 \to \gamma\gamma$, the low-energy singularities via $e^+e^- \to 2\pi, 3\pi$, spacelike data for large Q^2, and short-distance constraints—allows for a reliable evaluation of the long-range $\gamma^*\gamma^*$ contribution, leading to a SM prediction (19) with a precision of 0.5%. The loop integral can be reduced to standard loop functions by means of a double-spectral representation, for which also a Wick rotation to spacelike momenta becomes possible. The conceptual advances presented here will also become relevant for refined predictions of the dilepton decays of $\eta^{(\prime)}$.

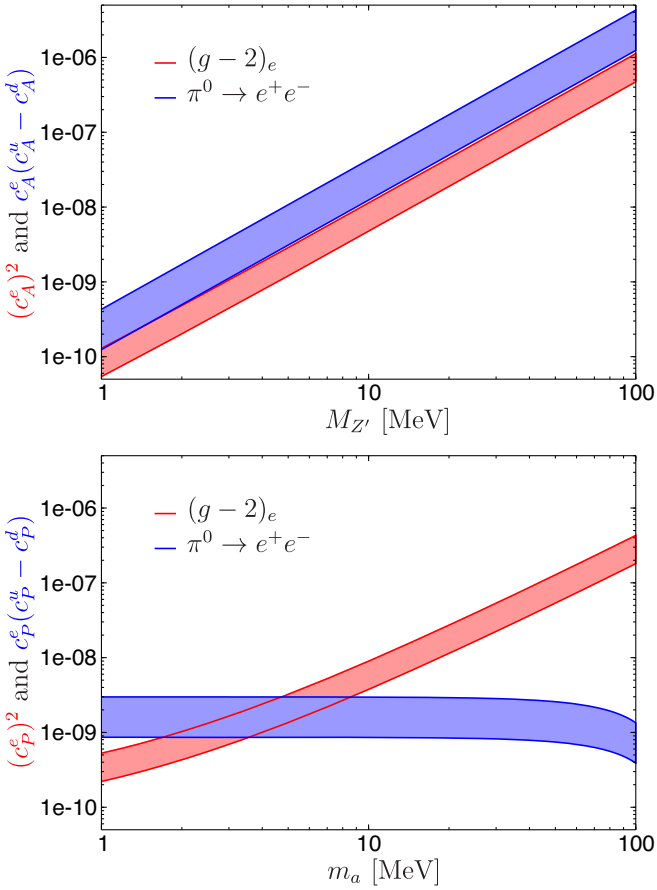

FIG. 3. 1σ parameter ranges preferred by $\Delta a_e[\mathrm{Cs}]$ (red) and $\pi^0 \to e^+e^-$ (blue) on the couplings of light axial-vector (upper) and pseudoscalar (lower) mediators.

By comparing our SM prediction to the KTeV measurement we then provided the corresponding constraints on axial-vector and pseudoscalar operators, both in SM effective field theory and for light mediators. In the latter case, we compared the (mildly) favored parameter space to the one suggested by the anomalous magnetic moment of the electron when contrasted to the fine-structure constant measured with Cs atom interferometry. With our calculation of the $\pi^0 \to e^+e^-$ width, the theoretical precision now exceeds experiment by an order of magnitude, allowing for concurrent advances in BSM constraints once an improved measurement becomes available. Such efforts are in progress at NA62 [117].

We thank Tomáš Husek, Karol Kampf, and Jiří Novotný for valuable communication regarding Refs. [40,41]. Financial support by the SNSF (Project No. PCEFP2_181117) and the DFG through the funds provided to the Sino-German Collaborative Research Center TRR110

"Symmetries and the Emergence of Structure in QCD" (DFG Project-ID 196253076–TRR 110) is gratefully acknowledged. J. L. is supported by the FWF-DACH Grant No. I 3845-N27 and by the FWF doctoral program Particles and Interactions, Project No. W 1252-N27.

[1] J. Wess and B. Zumino, Phys. Lett. **37B**, 95 (1971).
[2] E. Witten, Nucl. Phys. **B223**, 422 (1983).
[3] S. L. Adler, Phys. Rev. **177**, 2426 (1969).
[4] J. S. Bell and R. Jackiw, Nuovo Cimento A **60**, 47 (1969).
[5] W. A. Bardeen, Phys. Rev. **184**, 1848 (1969).
[6] P. A. Zyla *et al.* (Particle Data Group Collaboration), Prog. Theor. Exp. Phys. **2020**, 083C01 (2020).
[7] I. Larin *et al.* (PrimEx-II Collaboration), Science **368**, 506 (2020).
[8] J. Bijnens, A. Bramon, and F. Cornet, Z. Phys. C **46**, 599 (1990).
[9] B. Ananthanarayan and B. Moussallam, J. High Energy Phys. 05 (2002) 052.
[10] J. L. Goity, A. M. Bernstein, and B. R. Holstein, Phys. Rev. D **66**, 076014 (2002).
[11] K. Kampf and B. Moussallam, Phys. Rev. D **79**, 076005 (2009).
[12] T. Husek, K. Kampf, and J. Novotný, Phys. Rev. D **92**, 054027 (2015).
[13] M. Hoferichter, B. Kubis, S. Leupold, F. Niecknig, and S. P. Schneider, Eur. Phys. J. C **74**, 3180 (2014).
[14] M. Hoferichter, B.-L. Hoid, B. Kubis, S. Leupold, and S. P. Schneider, Phys. Rev. Lett. **121**, 112002 (2018).
[15] M. Hoferichter, B.-L. Hoid, B. Kubis, S. Leupold, and S. P. Schneider, J. High Energy Phys. 10 (2018) 141.
[16] P. Masjuan, Phys. Rev. D **86**, 094021 (2012).
[17] P. Masjuan and P. Sánchez-Puertas, Phys. Rev. D **95**, 054026 (2017).
[18] H. J. Behrend *et al.* (CELLO Collaboration), Z. Phys. C **49**, 401 (1991).
[19] P. Adlarson *et al.* (A2 Collaboration), Phys. Rev. C **95**, 025202 (2017).
[20] C. Lazzeroni *et al.* (NA62 Collaboration), Phys. Lett. B **768**, 38 (2017).
[21] T. Husek, E. Goudzovski, and K. Kampf, Phys. Rev. Lett. **122**, 022003 (2019).
[22] N. P. Samios, Phys. Rev. **121**, 275 (1961).
[23] M. A. Schardt, J. S. Frank, C. M. Hoffman, R. E. Mischke, D. C. Moir, and P. A. Thompson, Phys. Rev. D **23**, 639 (1981).
[24] A. Beddall, Eur. Phys. J. C **54**, 365 (2008).
[25] E. Abouzaid *et al.* (KTeV Collaboration), Phys. Rev. Lett. **100**, 182001 (2008).
[26] S. D. Drell, Nuovo Cimento **11**, 693 (1959).
[27] A. Soni, Phys. Lett. **52B**, 332 (1974).
[28] L. Arnellos, W. J. Marciano, and Z. Parsa, Nucl. Phys. **B196**, 365 (1982).
[29] P. Masjuan and P. Sánchez-Puertas, arXiv:1504.07001.
[30] P. Masjuan and P. Sánchez-Puertas, J. High Energy Phys. 08 (2016) 108.
[31] Y. Kahn, M. Schmitt, and T. M. P. Tait, Phys. Rev. D **78**, 115002 (2008).
[32] Y. Kahn, G. Krnjaic, S. Mishra-Sharma, and T. M. P. Tait, J. High Energy Phys. 05 (2017) 002.
[33] Q. Chang and Y.-D. Yang, Phys. Lett. B **676**, 88 (2009).
[34] S. Andreas, O. Lebedev, S. Ramos-Sánchez, and A. Ringwald, J. High Energy Phys. 08 (2010) 003.
[35] M. Bauer, M. Neubert, and A. Thamm, J. High Energy Phys. 12 (2017) 044.
[36] D. S. M. Alves and N. Weiner, J. High Energy Phys. 07 (2018) 092.
[37] W. Altmannshofer, S. Gori, and D. J. Robinson, Phys. Rev. D **101**, 075002 (2020).
[38] M. Bauer, M. Neubert, S. Renner, M. Schnubel, and A. Thamm, arXiv:2110.10698.
[39] E. Abouzaid *et al.* (KTeV Collaboration), Phys. Rev. D **75**, 012004 (2007).
[40] P. Vaško and J. Novotný, J. High Energy Phys. 10 (2011) 122.
[41] T. Husek, K. Kampf, and J. Novotný, Eur. Phys. J. C **74**, 3010 (2014).
[42] L. Bergström, Z. Phys. C **20**, 135 (1983).
[43] A. E. Dorokhov, E. A. Kuraev, Y. M. Bystritskiy, and M. Secansky, Eur. Phys. J. C **55**, 193 (2008).
[44] T. Husek, K. Kampf, and J. Novotný (private communication).
[45] S. Berman and D. Geffen, Nuovo Cimento **18**, 1192 (1960).
[46] M. Pratap and J. Smith, Phys. Rev. D **5**, 2020 (1972).
[47] L. Gan, B. Kubis, E. Passemar, and S. Tulin, Phys. Rep. **945**, 1 (2022).
[48] M. J. Savage, M. E. Luke, and M. B. Wise, Phys. Lett. B **291**, 481 (1992).
[49] D. Gómez Dumm and A. Pich, Phys. Rev. Lett. **80**, 4633 (1998).
[50] L. Ametller, A. Bramon, and E. Massó, Phys. Rev. D **48**, 3388 (1993).
[51] M. Knecht, S. Peris, M. Perrottet, and E. de Rafael, Phys. Rev. Lett. **83**, 5230 (1999).
[52] Z. K. Silagadze, Phys. Rev. D **74**, 054003 (2006).
[53] T. Husek and S. Leupold, Eur. Phys. J. C **75**, 586 (2015).
[54] L. Bergström, E. Massó, L. Ametller, and A. Bramon, Phys. Lett. **126B**, 117 (1983).
[55] L. Ametller, L. Bergström, A. Bramon, and E. Massó, Nucl. Phys. **B228**, 301 (1983).
[56] A. E. Dorokhov and M. A. Ivanov, Phys. Rev. D **75**, 114007 (2007).
[57] A. E. Dorokhov and M. A. Ivanov, JETP Lett. **87**, 531 (2008).
[58] A. E. Dorokhov, M. A. Ivanov, and S. G. Kovalenko, Phys. Lett. B **677**, 145 (2009).
[59] E. Weil, G. Eichmann, C. S. Fischer, and R. Williams, Phys. Rev. D **96**, 014021 (2017).
[60] G. Eichmann, C. S. Fischer, E. Weil, and R. Williams, Phys. Lett. B **774**, 425 (2017).
[61] J. Gronberg *et al.* (CLEO Collaboration), Phys. Rev. D **57**, 33 (1998).
[62] B. Aubert *et al.* (*BABAR* Collaboration), Phys. Rev. D **80**, 052002 (2009).
[63] S. Uehara *et al.* (Belle Collaboration), Phys. Rev. D **86**, 092007 (2012).
[64] N. H. Christ, X. Feng, L. Jin, C. Tu, and Y. Zhao, Proc. Sci., LATTICE2019 (**2020**) 097.

[65] M. Hoferichter, G. Colangelo, M. Procura, and P. Stoffer, Int. J. Mod. Phys. A **35**, 1460400 (2014).
[66] G. Colangelo, M. Hoferichter, M. Procura, and P. Stoffer, J. High Energy Phys. 09 (2014) 091.
[67] G. Colangelo, M. Hoferichter, B. Kubis, M. Procura, and P. Stoffer, Phys. Lett. B **738**, 6 (2014).
[68] G. Colangelo, M. Hoferichter, M. Procura, and P. Stoffer, J. High Energy Phys. 09 (2015) 074.
[69] G. Colangelo, M. Hoferichter, M. Procura, and P. Stoffer, Phys. Rev. Lett. **118**, 232001 (2017).
[70] G. Colangelo, M. Hoferichter, M. Procura, and P. Stoffer, J. High Energy Phys. 04 (2017) 161.
[71] I. Danilkin, M. Hoferichter, and P. Stoffer, Phys. Lett. B **820**, 136502 (2021).
[72] M. Hoferichter, B.-L. Hoid, and B. Kubis, J. High Energy Phys. 08 (2019) 137.
[73] B.-L. Hoid, M. Hoferichter, and B. Kubis, Eur. Phys. J. C **80**, 988 (2020).
[74] G. Colangelo, F. Hagelstein, M. Hoferichter, L. Laub, and P. Stoffer, Phys. Rev. D **101**, 051501(R) (2020).
[75] G. Colangelo, F. Hagelstein, M. Hoferichter, L. Laub, and P. Stoffer, J. High Energy Phys. 03 (2020) 101.
[76] M. Hoferichter and P. Stoffer, J. High Energy Phys. 05 (2020) 159.
[77] A. Gérardin, H. B. Meyer, and A. Nyffeler, Phys. Rev. D **100**, 034520 (2019).
[78] M. Knecht and A. Nyffeler, Phys. Rev. D **65**, 073034 (2002).
[79] W. Lucha, D. Melikhov, and S. Simula, Phys. Rev. D **75**, 016001 (2007); **92**, 019901(E) (2015).
[80] G. Colangelo, M. Hoferichter, and P. Stoffer, J. High Energy Phys. 02 (2019) 006.
[81] G. Colangelo, M. Hoferichter, and P. Stoffer, Phys. Lett. B **814**, 136073 (2021).
[82] N. N. Khuri and S. B. Treiman, Phys. Rev. **119**, 1115 (1960).
[83] G. P. Lepage and S. J. Brodsky, Phys. Lett. **87B**, 359 (1979).
[84] G. P. Lepage and S. J. Brodsky, Phys. Rev. D **22**, 2157 (1980).
[85] A. Khodjamirian, Eur. Phys. J. C **6**, 477 (1999).
[86] M. Zanke, M. Hoferichter, and B. Kubis, J. High Energy Phys. 07 (2021) 106.
[87] S. S. Agaev, V. M. Braun, N. Offen, and F. A. Porkert, Phys. Rev. D **83**, 054020 (2011).
[88] S. V. Mikhailov, A. V. Pimikov, and N. G. Stefanis, Phys. Rev. D **93**, 114018 (2016).
[89] See Supplemental Material at http://link.aps.org/supplemental/10.1103/PhysRevLett.128.172004 for more details on the evaluation of the loop integrals.
[90] J. Lüdtke, Bachelor's thesis, University of Bonn, 2016.
[91] B.-L. Hoid, Ph.D. thesis, University of Bonn, 2020, https://hdl.handle.net/20.500.11811/8906.
[92] J. L. Rosner, Ann. Phys. (Leipzig) **44**, 11 (1967).
[93] M. J. Levine and R. Roskies, Phys. Rev. D **9**, 421 (1974).
[94] M. J. Levine, E. Remiddi, and R. Roskies, Phys. Rev. D **20**, 2068 (1979).
[95] G. 't Hooft and M. J. G. Veltman, Nucl. Phys. **B153**, 365 (1979).
[96] T. Hahn and M. Pérez-Victoria, Comput. Phys. Commun. **118**, 153 (1999).
[97] P. Sánchez-Puertas, J. High Energy Phys. 01 (2019) 031.
[98] S. Aoki *et al.* (Flavour Lattice Averaging Group Collaboration), Eur. Phys. J. C **80**, 113 (2020).
[99] C. McNeile, C. T. H. Davies, E. Follana, K. Hornbostel, and G. P. Lepage, Phys. Rev. D **82**, 034512 (2010).
[100] S. Dürr, Z. Fodor, C. Hoelbling, S. D. Katz, S. Krieg, T. Kurth, L. Lellouch, T. Lippert, K. K. Szabo, and G. Vulvert, Phys. Lett. B **701**, 265 (2011).
[101] N. Carrasco *et al.* (European Twisted Mass Collaboration), Nucl. Phys. **B887**, 19 (2014).
[102] T. Blum *et al.* (RBC and UKQCD Collaborations), Phys. Rev. D **93**, 074505 (2016).
[103] A. Bazavov *et al.* (Fermilab Lattice, MILC, and TUMQCD Collaborations), Phys. Rev. D **98**, 054517 (2018).
[104] B. Grzadkowski, M. Iskrzyński, M. Misiak, and J. Rosiek, J. High Energy Phys. 10 (2010) 085.
[105] W. Buchmüller and D. Wyler, Nucl. Phys. **B268**, 621 (1986).
[106] J. de Blas, M. Chala, and J. Santiago, Phys. Rev. D **88**, 095011 (2013).
[107] A. Falkowski, M. González-Alonso, and K. Mimouni, J. High Energy Phys. 08 (2017) 123.
[108] A. Crivellin, M. Hoferichter, M. Kirk, C. A. Manzari, and L. Schnell, J. High Energy Phys. 10 (2021) 221.
[109] D. Hanneke, S. Fogwell, and G. Gabrielse, Phys. Rev. Lett. **100**, 120801 (2008).
[110] T. Aoyama, T. Kinoshita, and M. Nio, Atoms **7**, 28 (2019).
[111] T. Aoyama *et al.*, Phys. Rep. **887**, 1 (2020).
[112] R. H. Parker, C. Yu, W. Zhong, B. Estey, and H. Müller, Science **360**, 191 (2018).
[113] L. Morel, Z. Yao, P. Cladé, and S. Guellati-Khélifa, Nature (London) **588**, 61 (2020).
[114] J. P. Leveille, Nucl. Phys. **B137**, 63 (1978).
[115] J. Liu, C. E. M. Wagner, and X.-P. Wang, J. High Energy Phys. 03 (2019) 008.
[116] J. P. Lees *et al.* (*BABAR* Collaboration), Phys. Rev. Lett. **119**, 131804 (2017).
[117] NA62, 2020 NA62 Status Report to the CERN SPSC, https://cds.cern.ch/record/2713499 (2020).